Joshua D. Berwanger[+a], Melinda A. Lake[+b], Sanniv Ganguly[c], Junyan Yang[d], Christopher J. Welch[e], Jacqueline C. Linnes[c], and Merlin Bruening[*a,d]

[+] = equal contribution
[*] = corresponding author; mbruenin@nd.edu
[a] = Department of Chemistry and Biochemistry, University of Notre Dame, Notre Dame, Indiana 46556, United States
[b] = School of Mechanical Engineering, Purdue University, West Lafayette, Indiana, 47907, United States
[c] = Weldon School of Biomedical Engineering, Purdue University, West Lafayette, Indiana, 47907, United States
[d] = Department of Chemical and Biomolecular Engineering, University of Notre Dame, Notre Dame, Indiana 46556, United States
[e] = Indiana Consortium for Analytical Science and Engineering (ICASE), Indianapolis, Indiana, 46202, United States

ABSTRACT

Control of monoclonal antibody (mAb) concentrations in serum is important for maintaining the safety and efficacy of these lifesaving therapeutics. Point-of-care (POC) quantification of therapeutic mAbs could ensure that patients have effective mAb levels without compromising safety. This work uses mimotope-functionalized microporous alumina affinity membranes in vertical flow assays for detection and quantitation of therapeutic mAbs. Selective capture of bevacizumab from 1000:1 diluted serum or plasma and binding of a fluorescently labelled anti-human IgG secondary antibody enable fluorescence-based analysis of bevacizumab at its therapeutically relevant concentration range of ~50 to 300 μg/mL. The assay results in a linear relationship between the fluorescence intensity of the antibody capture spot and the bevacizumab concentration. A simple prototype microfluidic device containing these membranes allows washing, reagent additions and visualization of signal within 15 minutes using a total of 5 mL of fluid. The prototype devices can monitor physiologically relevant bevacizumab levels in diluted serum, and future refinements might lead to a POC device for therapeutic drug monitoring.

KEYWORDS: mimotopes, monoclonal antibodies (mAbs), therapeutic drug monitoring, vertical flow assays, point-of-care, microfluidics

INTRODUCTION

Pharmaceutical applications of monoclonal antibodies (mAbs) have grown at an astonishing rate since the introduction of the first therapeutic mAb in 1986.[1] As of April 2021, 100 therapeutic monoclonal antibodies were approved as treatments, and that number has grown since then, with mAbs accounting for almost a fifth of new approved drugs in the US.[1–4] mAb therapies are highly specific in treating inflammatory diseases, autoimmune diseases, pain, and cancers, but their efficacy often depends on maintaining the proper mAb concentration in blood.[5–10] For example, clinical pharmacokinetic studies showed a large patient-to-patient variation in the serum concentrations of two cancer therapeutics, bevacizumab and trastuzumab, at the same time point after mAb administration.[11–14] For both mAbs, the serum concentration affected the outcome of the treatment. In the case of trastuzumab and ado-trastuzumab (a drug conjugate), higher exposure to the drug correlated with higher drug efficacy while patients with lower exposure had shorter overall survival times.[10,15] With bevacizumab, higher survival chances correlated with higher mAb concentrations in both metastatic colon cancer and glioma, but in the case of glioma, side effects began to arise as the concentration of bevacizumab increased beyond 250 mg/L.[8,11] The inter-patient variability of pharmacokinetics is an unmet problem of the current standard dosage regimens that are based on body weight (mg/kg) or set dosages. Therapeutic drug monitoring could address the challenge of interpatient pharmacokinetic variability and inform personalized dosage regimens to increase the clinical effectiveness and potentially lower the cost of these treatments.[8,16] This approach has

shown effectiveness for several drug classes such as antibiotics, antiepileptics, and immunosuppressants, but its usage in therapeutic mAb treatment is still nascent. [16–23]

Ideally, therapeutic monitoring of mAbs will employ a fast and inexpensive method to determine their concentrations in patient blood. Current methods for mAb quantitation include enzyme-linked immunosorbent assays (ELISAs), liquid chromatography-mass spectrometry, and Single Molecular Array (SIMOA)/Luminex assays.[24–28] Although these techniques are sensitive and accurate, they require several time-consuming steps as well as expensive equipment in some cases. Thus, they are not applicable to point-of-care (POC) therapeutic drug monitoring.[29,30]

Vertical flow through membranes in microfluidic devices may afford rapid capture of targets to enable POC analyses. Many studies demonstrated the utility of flow through membranes in immunoassays.[31–33] Examples of such devices include a colorimetric method to detect *B. pseudomallei* down to 0.02 ng/mL in a nitrocellulose membrane,[34] and a fluorescence-based assay in a paper fluidic device to detect cancer biomarkers from 0.1-1000 ng/mL.[35] Additionally, researchers developed a POC device to monitor flucytosine uptake in a nitrocellulose membrane using gold nanoparticles to detect 10 µg/mL levels using surface enhanced Raman spectroscopy.[36] We demonstrated a microplate-based vertical flow assay that employs an epitope-mimicking peptide (mimotope) to quantify trastuzumab and a mAb for SARS-Cov-2 in less than 5 minutes.[37]

This study explores vertical-flow immunoassays to rapidly determine bevacizumab concentrations in patient blood plasma or serum using a macroscale fluidic device as well as a proof-of-concept microfluidic device designed to reduce both assay time and reagent volume. Building on recent work on the capture and analysis of therapeutic mAbs using microporous

membranes,[38] we employ a microfluidic workflow that utilizes membranes covalently modified with a mAb-binding mimotope [39] to capture and quantify target therapeutic mAbs in patient serum. Such membranes are attractive because they may efficiently capture mAbs in minutes (including rinsing steps). Importantly, quantitation of the mAbs via a fluorescently labelled secondary antibody allows detection bevacizumab at clinically relevant levels between ~60 and 300 ng/mL in 1000-fold diluted serum.[8,11] Our microfluidic chip that exploits vertical-flow capture consists of layers of plastic and pressure sensitive adhesive (PSA), making it low-cost and scalable through roll-to-roll manufacturing [40] or adaptable into an injection molded platform.[41] We integrate a functionalized porous alumina membrane within the adhesive and plastic layers. Thin, optically clear layers enable imaging of the membrane within the microfluidic chip, rendering the device adaptable to point-of-care smartphone-based imaging platforms.[42]

EXPERIMENTAL SECTION

Materials

Alumina membranes (Whatman Anodisc inorganic filter membranes, 25 mm diameter, 0.2 □m pore size) were cleaned in a UV/O_3 chamber (Jelight, model 18) for 15 minutes prior to use. Acetyl-WLEMHWPAHSGSGSGSK (Bev17, the mimotope that binds to bevacizumab) was synthesized by Genscript with a purity greater than 95%. Polyallylamine hydrochloride (PAH, Mw= 50,000), poly(acrylic acid) (PAA, average molecular weight ~100,000 Da, 35% aqueous solution), Tween-20 surfactant, N-hydroxysuccinimide (NHS), N-(3-dimethylaminopropyl)-N'-ethylcarbodiimide hydrochloride (EDC), and human serum were used as received from Sigma Aldrich. BioChemEd Services provided deidentified patient serum samples. Human blood was received from Innovative Research in a sodium citrate anti-coagulant tube and centrifuged at

2000xg for 10 minutes before extracting plasma using a pipette. Poly(vinyl) alcohol (PVA, 99–100% hydrolyzed, approximate molecular weight 8600 Da) was obtained from Acros. Bevacizumab (Genentech) was used from its therapeutic formulations. Buffers were prepared using analytical grade chemicals from various chemical providers, and Milli-Q, 18.2 M cm deionized water was used to prepare all aqueous solutions. Two Wash buffers used throughout the assays were prepared. Wash Buffer 1 is a solution containing 20 mM PBS, 500 mM NaCl, and 0.1 % (v/v) Tween 20 (pH 7.2). Wash Buffer 2 is a solution containing 20 mM PBS, 500 mM NaCl, 0.1% Tween 20, and 0.1% PVA at (pH 7.2). PVA was added to remove non-specifically bound proteins.

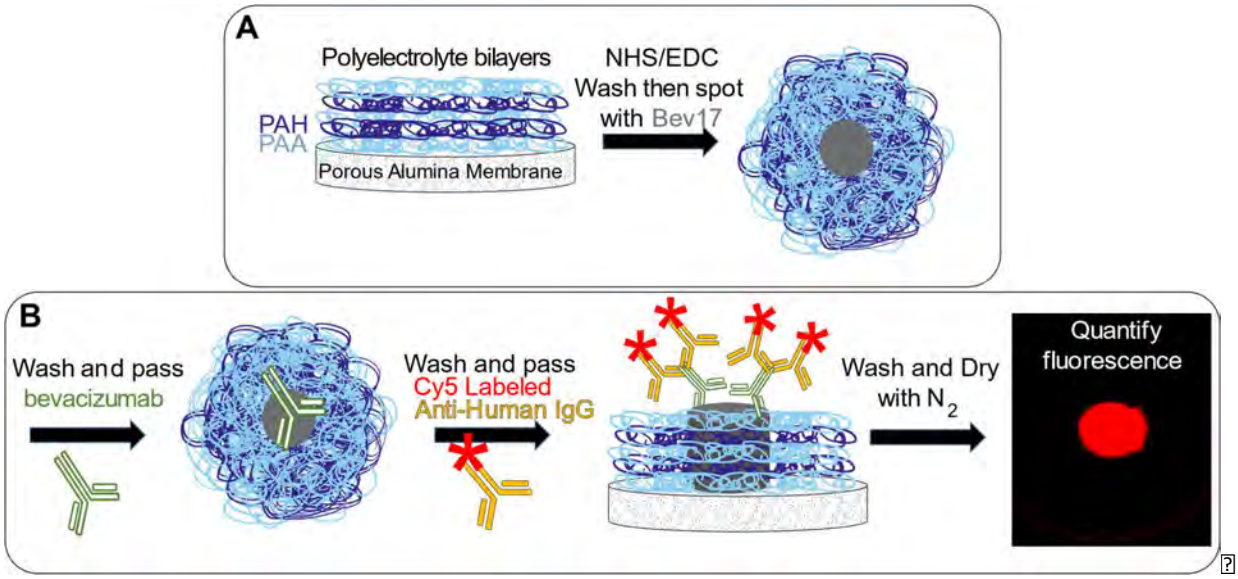

Figure 1. Alumina membrane modification and steps of a flow assay. A) Modification of a polyelectrolyte-coated alumina membrane with peptide mimotopes. Polyelectrolyte deposition, mimotope spotting, and mAb capture occur throughout the alumina substrate. B) Capture and analysis of bevacizumab using mimotope-modified alumina membranes and binding of a fluorescently labelled secondary antibody.

Modification of Bare Alumina Membranes with Peptide Mimotopes

Layer-by-layer adsorption was employed to modify alumina membranes (Figure 1A).[43] UV/O_3-cleaned membranes were washed with water prior to immersion in a PAA solution (10

mM of the PAA repeating unit in 500 mM aqueous NaCl, pH 4) for 5 min. The membranes were then immersed sequentially in deionized water for 1 min, PAH solution for 5 min (10 mM of the PAH repeating unit in aqueous 500 mM NaCl, pH 4), and deionized water for 1 min. This process was repeated until the membrane was modified with the desired number of polyelectrolyte bilayers (1.5, 2.5, or 3.5; the extra 0.5 bilayer indicates that the film ends in PAA). The membranes were then dried gently with N_2 gas. After drying, the $(PAA/PAH)_xPAA$-modified alumina membranes were rinsed with water for 10 seconds on both sides and immersed in a 0.1 M NHS, 0.1 M EDC aqueous solution for 30 min. The activated membranes were again rinsed with water for 10 seconds on either side and dried with N_2 gas. Next, 0.75 µL of Bev17 mimotope peptide (1 mg/mL in 0.1 M $NaHCO_3$, pH 9) was pipetted onto the middle of the membrane. The membranes were then placed in covered polystyrene petri dishes saturated with water vapor by a cotton ball swab to allow covalent immobilization of Bev17 overnight. Note that the poly(acrylic acid) modification occurs over the entire membrane, so only Bev17 binding and subsequent mAb capture should affect flow through the spot relative to the rest of the porous alumina. Membranes used in the microfluidics assay were shipped overnight on ice and stored in a 4°C refrigerator upon arrival.

Capture and Analysis of Bevacizumab with Mimotope-Modified Alumina Membranes

After letting Bev17-modified alumina membranes sit overnight at room temperature, the membranes were used in an antibody capture assay (Figure 1B) in a custom-built Teflon vertical flow device that holds the membrane, as detailed elsewhere.[44–46] The membranes were rinsed for 10 seconds on each side with water. Membrane testing employed a peristaltic pump (HV-77120-62 Masterflex, Gelsenkirchen, GER) to pull fluid from an inlet reservoir through the membranes. The pump is connected via tubing to the outlet of the membrane holder. After

placing a membrane in a Teflon holder, it was rinsed by flowing 30 mL of Wash Buffer 1 through the membrane at 1 mL/min using the peristaltic pump. Next, 1 mL of bevacizumab at concentrations ranging from 0 to 500 ng/mL in 20 mM PBS, 150 mM NaCl, pH 7.4 was circulated through the membrane for varying amounts of time from 1 to 10 min at 1 mL/min. The membranes were then washed with varying volumes between 5 and 30 mL of Wash Buffer 1. After washing, 1 mL of Cy5-labelled Anti-Human IgG (10 µg/mL in 20 mM PBS, 500 mM NaCl, pH 7.4) was circulated through the membrane at 1 mL/min for varying amounts of time between 10 min and 50 min. The membranes were then washed again with Wash Buffer 1, removed from the pump setup, rinsed with water for 10 seconds on each side, dried with N_2 gas, and analyzed using an Azure C400 Bioanalytical Imaging System in the Cy5 imaging mode using a 50 ms exposure time. Quantitation of the images was carried out using the ImageJ intensity measurement function by integrating the intensity over the area of a circle of 4.9 mm^2 that fit within the edges of the mimotope spots. The circle size was determined by finding the area that fit within the spots on all the membranes analyzed in that data set. The fluorescence intensity was reasonably uniform across the spots (see Figure S4 in the supporting information).

After developing conditions for capture and analysis of bevacizumab in buffer, the process was repeated using mAb spiked in human fluids. Experiments were repeated with both human serum and human plasma. The human fluids were first diluted 1000:1 with a solution containing 20 mM PBS and 500 mM NaCl at pH 7.4. These diluted samples were then spiked with a known amount of the target bevacizumab at concentrations ranging from 0 to 500 ng/mL. The Bev17-spotted membranes were pretreated with Wash Buffer 1 as described above. After pretreatment, 1 mL of the bevacizumab-spiked, diluted human fluid was passed once through the membrane at 1 mL/min to capture the target. After capture, the membranes were washed with varying volumes

between 5 to 30 mL of Wash Buffer 2. After washing, 1 mL of Cy5-labelled Anti-Human IgG (1-10 µg/mL in 20 mM PBS, 500 mM NaCl, pH 7.4) was circulated through the membrane at 1 mL/min for 10 minutes. Membranes were washed again with Wash Buffer 2, rinsed, dried, and analyzed as described above using fluorescence imaging. The membranes were also imaged on an inverted microscope (Zeiss Axio Observer Z1, Carl Zeiss Microscopy, Jena, Germany) in brightfield mode using the 5X-20X objectives to inspect for cracks.

Bevacizumab capture in a microfluidic device

Device fabrication

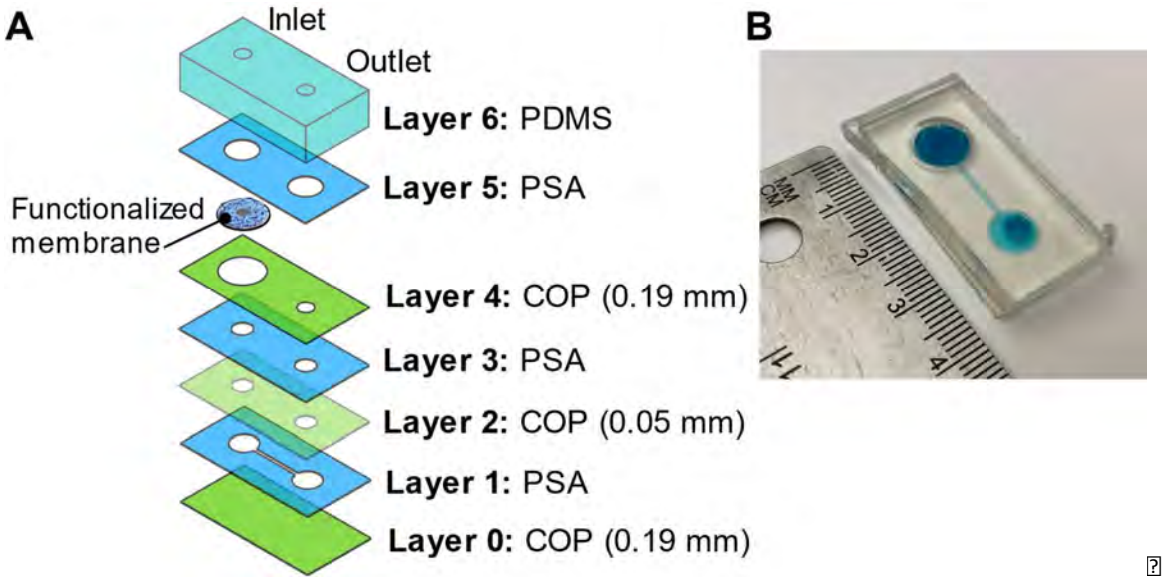

Figure 2. A) Exploded view of the microfluidic device assembly. B) Photograph of an assembled chip filled with blue food coloring. COP= cyclic olefin polymer. PSA = pressure sensitive adhesive. PDMS= polydimethylsiloxane.

Microfluidic devices were designed in AutoCAD, and the files were transferred to Adobe Illustrator for production. Each device contained six layers: 2 layers of 0.19 mm-thick cyclic olefin polymer (COP) (Zeonor, Tokyo, Japan), 1 layer of 0.05 mm-thick COP, 3 layers of PSA (93020LE, 3M, St. Paul, MN, USA), and 1 layer of polydimethylsiloxane (PDMS) (Sylgard 184, Dow Corning, Midland, MI, USA) (Figure 2). Each plastic and adhesive layer of the chip was

cut using a laser cutter (VLS3.50, Universal Laser Systems Inc., Scottsdale, AZ, USA) and assembled manually. COP was cut using a laser power of 80% and a speed of 100%, and the PSA was cut using a laser power of 90% with a speed of 90%. The membranes have an initial diameter of 25 mm prior to laser cutting and have an outer ring of plastic that provides a protective border for gripping the membrane. The 25-mm membrane with an antibody spot was laser cut to 10 mm using a laser power of 56% and a speed of 80%. Laser cutting removes the protective plastic ring, so afterward the membrane is directly handled with tweezers. Chip assembly could be scaled to a roll-to-roll manufacturing setup or adapted into an injection moldable design. The PDMS layer is added to secure the PEEK tubing (Part 1569, Idex Health & Science, Oak Harbor, WA, USA) to the inlet and outlet. PDMS was fabricated using a 10:1 base:curing agent ratio, baked in a petri dish for 2 hours at 65° C, and hole punched and diced to size after curing. The COP pieces were rinsed with 70% v/v ethanol in water and dried using a Kimwipe prior to assembly. Layer 0 to Layer 4 were assembled and stored at room temperature for up to two weeks, while Layers 5 and 6 were assembled on the day of the experiment following placement of the alumina membrane in the pre-designed slot in layer 4.

Microfluidic device assay

In binding studies for the microfluidic device assay, all solutions were passed over the membrane through the chip with a syringe pump (Part 788212, KD Scientific, Holliston, MA) connected to the inlet to maintain a constant flowrate and a measurable residence time for interaction. The outlet side had a tube connected to a waste container. The binding was performed in 3 separate sets of trials evaluating the dose-dependent fluorescence in response to various concentrations of bevacizumab spiked into serum. Trial 1 and Trial 2 were tested out of the same prepared membrane batch: Trial 1 occurred within 2 days of membrane delivery and

Trial 2 occurred 1 week later. Trial 3 was tested within 2 days of delivery of a new batch of membranes. After sealing the laser-cut alumina into the device, the modified alumina membrane within the chip was first washed with 0.8 mL of Wash buffer 1 at a constant flow rate of 1 mL/min, followed by running the 1000:1 diluted serum with 20 mM PBS and 500 mM NaCl at pH 7.2 spiked with varying concentrations of bevacizumab from 0 to 300 ng/mL at a flow rate of 0.5 mL/min with a volume of 0.16 mL. This was followed by washing the membrane with 0.8 mL of Wash Buffer 2. Goat Anti-Human IgG H&L (Cy5 ®) (Abcam) was then diluted to 1 µg/mL in 20 mM PBS, 500 mM NaCl, pH 7.4, and 0.6 mL of this dilute secondary antibody solution was flowed through the membrane for 10 minutes at 0.06 mL/min. This was followed by washing the membrane with 0.8 mL of Wash Buffer 2 and rinsing with 0.8 mL of deionized water, both at 1 mL/min. The tubing and pump were disconnected, then the PDMS layer was peeled off and the membranes were dried with N_2, but not removed from within the device. The membranes were then imaged from the top in the Azure c600 fluorescence imager (Azure Biosystems, Dublin, CA, USA) in the Cy5 mode with a 50 ms exposure time. The contrast settings of the Azure scanner were adjusted to the same black/white values of 0/6242 $\pm$ 23 a.u. for the 3 trials to make the spots bright enough to see and yet avoid saturation of the fluorescence. The small deviation in the setting is due to the machine options. Quantitation of the images was carried out using the ImageJ intensity measurement function by integrating the intensity over the area of a 1.5 mm^2 circle that fit within the edges of the mimotope spot. The circle size was determined by finding the area that fit within the spots on all the membranes analyzed in that data set.

RESULTS AND DISCUSSION

Mimotope-Modified Alumina Membranes for Analysis of Bevacizumab in Human Samples

This study uses fluorescence-based detection from porous alumina membranes with a total analysis time of less than 35 minutes in a membrane holder and only 15 min in a microfluidic device. The long optical pathlength in alumina membranes provides up to two orders of magnitude greater sensitivity relative to assays using flat surfaces, allowing for shortened assay times.[43] Our prior work demonstrated mAb capture in modified nylon membranes, quantitation based on native mAb fluorescence, and preliminary use of a fluorescent secondary antibody to increase sensitivity with an analysis time of approximately 2 hrs.[47] Decreasing the assay time to 35 min requires optimization of all protocol steps including target antibody capture, washing, and secondary antibody capture. Initially, we studied analysis of mAbs in buffer to select the parameters for subsequent assays in serum and plasma. The Supporting Information describes our choices of times for each step of the analysis (Figures S1, S2, and Table S1) in large membrane holders. The final assay configuration includes a single pass of 1 mL of the primary mAb Bevacizumab through the 4.9-cm^2 membrane, 5 mL washing steps that occur after capture of the primary and secondary antibodies, and 10 min of secondary antibody circulation. These parameters represent a compromise between minimal analysis times and achieving high fluorescence signals with low background. All membranes are designed for single use due to their fragility and a desire to avoid contamination.

After selecting parameters for bevacizumab assays in buffer, we examined bevacizumab-spiked samples in diluted human serum or plasma using the same parameters. With a 1000-fold dilution, the serum or plasma components had minimal effect on bevacizumab binding to the mimotope on the alumina membrane. Removal of non-specifically bound proteins occurs during a wash step prior to capture of a secondary antibody as well as a final rinse; the PVA added to Wash Buffer 2 aids in removing excess proteins. Figure 3A shows results from the analysis of

bevacizumab in 1000-fold diluted serum. This 0-300 ng/mL assay range corresponds to the therapeutically relevant bevacizumab concentrations that would be present in 1000:1 diluted serum from patients.[8,11] The figure shows a linear relationship between the concentration of bevacizumab flowed through the membrane and the fluorescence intensity. Equally important, the background signal for 0 ng/mL of bevacizumab is low, indicating that under these conditions the 5-mL wash removes essentially all non-specifically bound secondary antibody. The low signal with no added bevacizumab also confirms that the signals observed on the other spots arise from the secondary antibody binding to bevacizumab and not from other proteins. The relatively large standard deviations in Figure 3B likely stem from the challenge of exactly reproducing the membrane preparation, particularly the spotting process, which was performed by hand. Nevertheless, the fluorescence values over the range from 100 to 300 ng/mL have a coefficient of variation (CV) less than 22%, with 80% having a CV of 20% or less. These uncertainties would likely be reduced further with standardization of membrane preparation to inform physicians about patient mAb levels in diluted serum. In particular, the spot size varies as much as 13% from the average spot size in 3 replicate measurements with the different concentrations for macroscale tests (Table S2) and 14% for the microfluidic tests described below (Table S3).

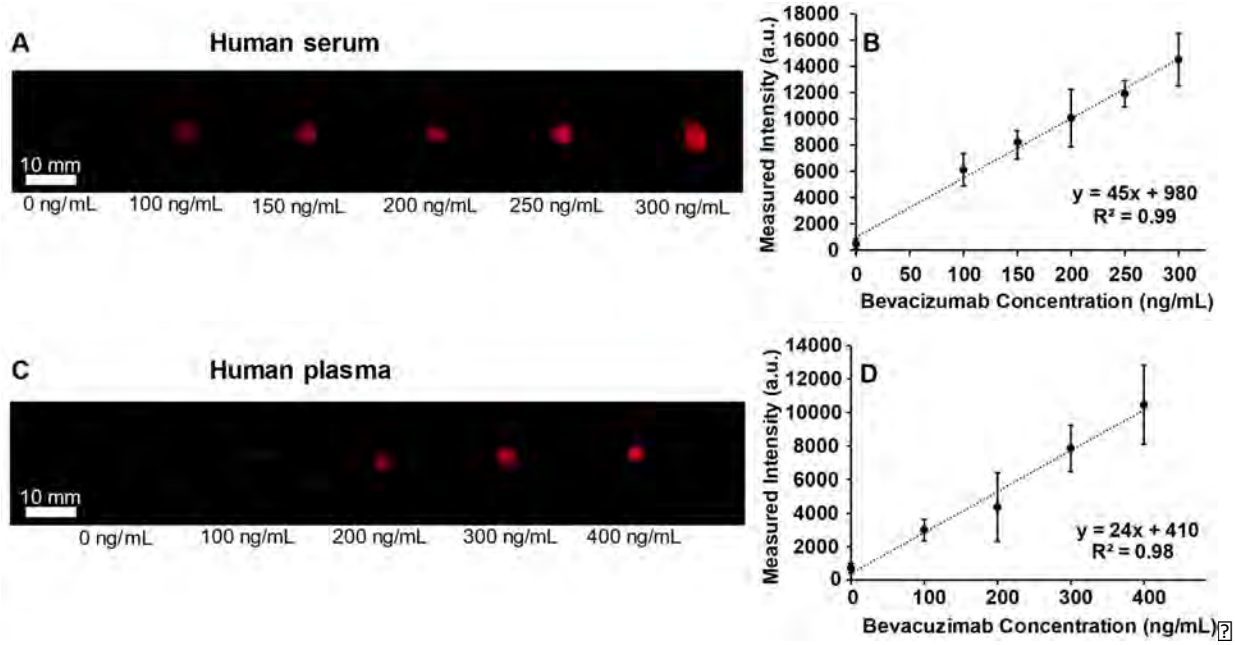

Figure 3. Analysis of bevacizumab in diluted human serum and diluted human plasma. A) Contrast-enhanced fluorescence image of Bev17-spotted $(PAA/PAH)_3PAA$-modified membranes after capture of bevacizumab from the diluted serum containing the indicated mAb concentration, rinsing, passage of a fluorescent secondary antibody, and further rinsing. B) Average intensity of spotted capture membranes as a function of bevacizumab concentration for the treatment described in A. The points on the line in panel B show the average measured intensity from 4 different membranes prepared on different days for each different concentration. C) Contrast-enhanced fluorescence image of Bev17-spotted (PAA/PAH)PAA-modified membranes after capture of Bevacizumab from diluted plasma containing the indicated mAb concentration, rinsing, passage of a fluorescent secondary antibody, and further rinsing. D) Average intensity of spotted capture membranes as a function of bevacizumab concentration for the treatment described in C. The points on the line in panel B show the average measured intensities from 3 different membranes prepared on different days at each different concentration. The error bars correspond to the standard deviations.

The results in Figure 3A and B employed $(PAA/PAH)_3PAA$ films for membrane modification, following a literature procedure.[43] We also tested the assay with $(PAA/PAH)_2PAA$ and (PAA/PAH)PAA films to decrease the transmembrane pressure, increase porosity, and facilitate incorporation of the membranes into a microfluidics device. Preliminary testing in the microfluidic devices with a $(PAA/PAH)_3PAA$-modified alumina resulted in cracked membranes and burst bonds between device layers due to the high pressures. Figure S3A shows that the background points for 0 ng/mL bevacizumab for membranes modified with $(PAA/PAH)_2PAA$ and (PAA/PAH)PAA films also showed minimal signals. Moreover, as Figure S3B-C show, the relationship between fluorescence intensity and the bevacizumab concentration

in 1000:1 diluted serum is linear for membranes modified using $(PAA/PAH)_2PAA$ and (PAA/PAH)PAA films. Thus, we proceeded with membranes coated with (PAA/PAH)PAA films because they show a linear response, low background, and relatively low back pressure.

Similar assays with spiked, diluted human plasma also show a linear relationship between the measured fluorescence intensity and the concentration of bevacizumab in solutions passed through the membrane (Figure 3C). There are three major differences in this assay compared to the procedure for the diluted serum. First, the assay with plasma required double the washing volume (10 mL vs 5 mL) to sufficiently remove non-specific binding. Second, to achieve sufficient sensitivity the assay required 10 µg/mL of the Cy5 labeled anti-human IgG, whereas the serum assay only need 1 µg/mL. The plasma has an anticoagulant and thus a different composition than the serum including proteins, calcium, and magnesium levels that may cause higher background or interactions with the bevacizumab/Bev17 that interfere with binding.[48] Nonetheless, the assay still exhibits the needed sensitivity while taking less than 35 minutes to complete. Based on the current standard deviations, the assay affords a coefficient of variation below 23%, except the 200 ng/mL point which has a much larger standard deviation (Figure 3D). The standard deviations are relatively large, but automated production of the membranes with precise spot placement and calibration of fluorescence using standards can likely overcome this challenge to reduce the errors to less than 20%.

As a comparison, we performed trastuzumab ELISAs in buffer using commercial kits and the manufacturer's protocols. With a commercial human IgG assay, the coefficient of variation was 10-20% when using 0.5 to 10 ng/mL and an assay time of 90 min. An anti-Her2 ELISA kit showed a coefficient of variation of 5% with concentrations from 10-100 ng/mL and an assay time of 120 min. Figure S5 in the supporting material shows calibration curves. Detection limits

were 0.2 ng/mL for the human IgG assay and 1.4 ng/mL for the anti-Her2 assay. Bevacizumab ELISA kits have a limit of quantitation around 30 ng/mL.[49] The ELISAs take at least an hour longer than the membrane-based method, and the human IgG assay shows similar uncertainty as the membrane-based system. ELISA detection limits are 2 orders of magnitude lower than those with the current membrane system. However, typical bevacizumab therapeutic concentrations are in the range of 50-300 µg/mL,[11] so low detection limits are not needed for this mAb. The main advantage of the membrane-based assays is a reduction in time, which we aim to decrease further in the future. Changes in the fluorophore on the secondary antibody should also decrease detection limits in the membrane-based assays.

Incorporation of Mimotope-Modified Membranes in a Microfluidic Chip

After developing analyses of bevacizumab in serum and plasma, the assay was miniaturized into a microfluidic workflow. The advantages of microfluidics include a decreased assay time, smaller reagent volumes, further method simplification, and the potential for automation, which could be valuable for future clinical use. Importantly, in a microfluidic device format this assay occurred in under 15 minutes and used a total of 4 mL of fluid, including the wash buffer and rinsing water. Thus, the prototype microfluidic assay demonstrates greater than 5X reduction in the reagent volumes compared to the standard assay. Other refinements may further decrease the required volumes to make this device more compatible with point of care diagnostics. Techniques such as ELISA employ small volumes, but they typically require >1 h for analysis and a plate reader for quantitation.

Figure 4 shows that for a given set of replicate experiments the fluorescence generally increases linearly with an increasing concentration of bevacizumab. Also, the background fluorescence in the membrane and the surrounding microfluidic chip is low compared to the

fluorescent spot at the center of the membrane (Figure 4A). The control without bevacizumab confirms the specificity of binding of the secondary antibody to bevacizumab.

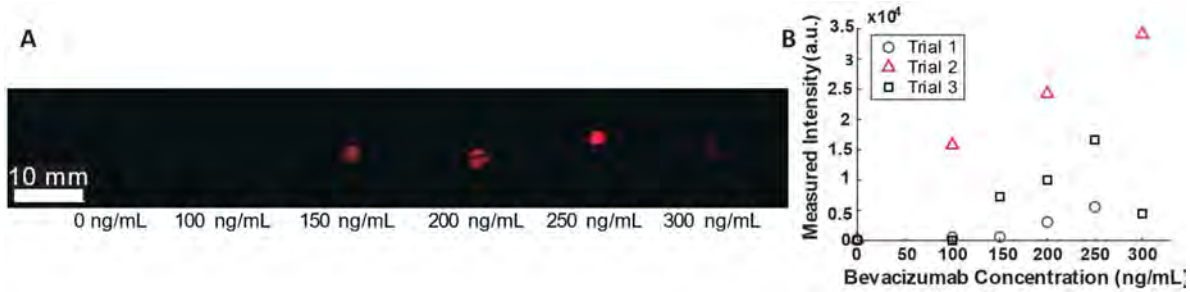

Figure 4. Analysis of bevacizumab in diluted (1000:1) human serum using a microfluidic assay. A) Contrast-enhanced fluorescence image of Bev17-spotted membranes after capture of bevacizumab from the diluted serum containing the indicated mAb concentration, rinsing, passage of a fluorescent secondary antibody, and further rinsing. B) Raw data collected for each membrane tested in the microfluidic system, excluding cases where membrane cracks were discovered. Each point represents a different membrane. The image in panel A corresponds to Trial 3 and was contrast-enhanced to increase visibility of the spots.

The fairly large differences in fluorescence intensities between different replicate measurements at the same bevacizumab concentrations may stem from variations in membrane preparation, or shipping conditions. For example, the alumina material is brittle and despite careful handling with tweezers, may develop microscopic or difficult to see cracks during device assembly. Such cracks will affect the assay by altering the flow-through properties of the membrane. After laser cutting the membranes down to 10 mm, the protective plastic ring is removed and thus the edge of the brittle membrane is directly handled with tweezers. When cracks were detected on a microscope, data points were dropped for Trial 2 at 150 and 250 ng/mL and Trial 1 at 300 ng/mL. Membranes used in the microfluidic assay were shipped on ice from Notre Dame to Purdue, so they had different storage conditions than the membranes fabricated and directly tested at Notre Dame. However, the microfluidic assay still demonstrates an approximately linear trend for each trial run with increasing bevacizumab concentration. Further, the manual spotting process for placing the spot at the center of the membrane in addition to different membrane storage times may add to variability in the microfluidic assay

results. This could be ameliorated with automated membrane production including precise spot placement. However, the signal areal intensity did not show a correlation with spot size (see Figure S6). Calibration of the fluorescence using standards integrated into the assay may also help future quantification. Further work is needed to increase reproducibility. With significant refinement, the microfluidic assay could allow simple point-of-care analyses that do not require the instrumentation currently required in assays that employ 96-well plates.

CONCLUSIONS

This study demonstrated fluorescence-based bevacizumab quantitation at therapeutically relevant ranges in diluted serum and plasma with porous alumina membranes. Preliminary results indicate that the process can occur in less than 15 minutes in a microfluidic device. In the macroscale and microfluidic vertical flow assays, the fluorescence signal varies approximately linearly with the concentration of bevacizumab. Moreover, the low signal with no added mAb confirms the high specificity of the assay. The study shows promise for a microfluidic antibody analysis platform. A scalable method to prepare the membranes should further improve reproducibility with lower errors. Additionally, calibration of the fluorescence using a standard could improve measurement consistency. Scaling the microfluidic platform through roll-to-roll manufacturing or injection molding would enable implementation of a low-cost POC device. Such a device may enable healthcare workers to rapidly measure therapeutic concentrations to ensure patients have effective mAb levels.

CONFLICT OF INTEREST

The authors declare that they have no known conflict of interests.

AUTHOR CONTRIBUTIONS

Joshua Berwanger: conceptualization, methodology, validation, formal analysis, investigation, and writing – original draft and review and editing. Melinda Lake: conceptualization, methodology, validation, formal analysis, investigation, and writing – original draft and review and editing. Sanniv Ganguly: formal analysis, investigation, writing – original draft and review and editing. Junyan Yang: methodology and validation; Christopher Welch: supervision, project administration, writing – original draft and review and editing. Jacqueline Linnes: conceptualization, supervision, project administration, writing – review and editing, and funding acquisition. Merlin Bruening: conceptualization, supervision, project administration, writing – review and editing, and funding acquisition.

ACKNOWLEDGEMENTS

We acknowledge funding from the NSF IUCRC Center for Bioanalytical Metrology (IIP 1916601 and IIP 1916691) and the Purdue University Lillian Gilbreth Postdoctoral Fellowship. The authors thank Ivan Budyak (Lilly) and Brandy Verhalen (Corteva Agriscience) for their technical expertise throughout the project. The authors also thank Muthu Meiyappan, and Christoph Zlabinger (Takeda) and Samin Akbari (Sartorius) for their technical expertise.

REFERENCES

[1] R.-M. Lu, Y.-C. Hwang, I.-J. Liu, C.-C. Lee, H.-Z. Tsai, H.-J. Li, H.-C. Wu, Development of therapeutic antibodies for the treatment of diseases, J. Biomed. Sci. 27 (2020) 1. https://doi.org/10.1186/s12929-019-0592-z.

[2] Homepage of The Antibody Society, Antib. Soc. https://www.antibodysociety.org/home/ (accessed May 13, 2022).

[3] A. Mullard, FDA approves 100th monoclonal antibody product, Nat. Rev. Drug Discov. (2021). https://doi.org/10.1038/d41573-021-00079-7.

[4] S.S. Wang, Y. (Susie) Yan, K. Ho, US FDA-approved therapeutic antibodies with high-concentration formulation: summaries and perspectives, Antib. Ther. 4 (2021) 262–272. https://doi.org/10.1093/abt/tbab027.

[5] S. Singh, N.K. Tank, P. Dwiwedi, J. Charan, R. Kaur, P. Sidhu, V.K. Chugh, Monoclonal antibodies: a review, Curr. Clin. Pharmacol. 13 (2018) 85–99. https://doi.org/10.2174/1574884712666170809124728.

[6] M. Berger, V. Shankar, A. Vafai, Therapeutic applications of monoclonal antibodies, Am. J. Med. Sci. 324 (2002) 14–30. https://doi.org/10.1097/00000441-200207000-00004.
[7] C.L.M. Krieckaert, S.C. Nair, M.T. Nurmohamed, C.J.J. van Dongen, W.F. Lems, F.P.J.G. Lafeber, J.W.J. Bijlsma, H. Koffijberg, G. Wolbink, P.M.J. Welsing, Personalised treatment using serum drug levels of adalimumab in patients with rheumatoid arthritis: an evaluation of costs and effects, Ann. Rheum. Dis. 74 (2015) 361–368. https://doi.org/10.1136/annrheumdis-2013-204101.
[8] A. Papachristos, P. Kemos, H. Kalofonos, G. Sivolapenko, Correlation between bevacizumab exposure and survival in patients with metastatic colorectal cancer, The Oncologist. (2020). https://doi.org/10.1634/theoncologist.2019-0835.
[9] A.L. Quartino, C. Hillenbach, J. Li, H. Li, R.D. Wada, J. Visich, C. Li, D. Heinzmann, J.Y. Jin, B.L. Lum, Population pharmacokinetic and exposure–response analysis for trastuzumab administered using a subcutaneous "manual syringe" injection or intravenously in women with HER2-positive early breast cancer, Cancer Chemother. Pharmacol. 77 (2016) 77–88. https://doi.org/10.1007/s00280-015-2922-5.
[10] J. Yang, H. Zhao, C. Garnett, A. Rahman, J.V. Gobburu, W. Pierce, G. Schechter, J. Summers, P. Keegan, B. Booth, Y. Wang, The combination of exposure-response and case-control analyses in regulatory decision making, J. Clin. Pharmacol. 53 (2013) 160–166. https://doi.org/10.1177/0091270012445206.
[11] G. Nugue, M. Bidart, M. Arlotto, M. Mousseau, F. Berger, L. Pelletier, Monitoring monoclonal antibody delivery in oncology: the example of bevacizumab, PLOS ONE. 8 (2013) e72021. https://doi.org/10.1371/journal.pone.0072021.
[12] J. Baselga, X. Carbonell, N.-J. Castañeda-Soto, M. Clemens, M. Green, V. Harvey, S. Morales, C. Barton, P. Ghahramani, Phase II study of efficacy, safety, and pharmacokinetics of trastuzumab monotherapy administered on a 3-weekly schedule, J. Clin. Oncol. 23 (2005) 2162–2171. https://doi.org/10.1200/JCO.2005.01.014.
[13] R. Bruno, C.B. Washington, J.-F. Lu, G. Lieberman, L. Banken, P. Klein, Population pharmacokinetics of trastuzumab in patients with HER2+ metastatic breast cancer, Cancer Chemother. Pharmacol. 56 (2005) 361–369. https://doi.org/10.1007/s00280-005-1026-z.
[14] D. Ternant, N. Cézé, T. Lecomte, D. Degenne, A.-C. Duveau, H. Watier, E. Dorval, G. Paintaud, An enzyme-linked immunosorbent assay to study bevacizumab pharmacokinetics, Ther. Drug Monit. 32 (2010) 647–652. https://doi.org/10.1097/FTD.0b013e3181ef582a.
[15] J. Wang, P. Song, S. Schrieber, Q. Liu, Q. Xu, G. Blumenthal, L. Amiri Kordestani, P. Cortazar, A. Ibrahim, R. Justice, Y. Wang, S. Tang, B. Booth, N. Mehrotra, A. Rahman, Exposure-response relationship of T-DM1: insight into dose optimization for patients with HER2-positive metastatic breast cancer, Clin. Pharmacol. Ther. 95 (2014) 558–564. https://doi.org/10.1038/clpt.2014.24.
[16] D.J. Touw, C. Neef, A.H. Thomson, A.A. Vinks, Cost-Effectiveness of Therapeutic Drug Monitoring, Ther Drug Monit. 27 (2005) 8. https://doi.org/10.1097/00007691-200502000-00004.
[17] W. Darko, J.J. Medicis, A. Smith, R. Guharoy, D.F. Lehmann, Mississippi mud no more: cost-effectiveness of pharmacokinetic dosage adjustment of vancomycin to prevent nephrotoxicity, Pharmacother. J. Hum. Pharmacol. Drug Ther. 23 (2003) 643–650. https://doi.org/10.1592/phco.23.5.643.32199.
[18] T.E. Welty, A.K. Copa, Impact of vancomycin therapeutic drug monitoring on patient care:, Ann. Pharmacother. (2016). https://doi.org/10.1177/106002809402801201.

[19] M.J. Eadie, The Role of therapeutic drug monitoring in improving the cost effectiveness of anticonvulsant therapy, Clin. Pharmacokinet. 29 (1995) 29–35. https://doi.org/10.2165/00003088-199529010-00004.
[20] S.I. Johannessen, D. Battino, D.J. Berry, M. Bialer, G. Krämer, T. Tomson, P.N. Patsalos, Therapeutic drug monitoring of the newer antiepileptic drugs, Ther. Drug Monit. 25 (2003) 347–363. https://doi.org/10.1097/00007691-200306000-00016.
[21] L.M. Shaw, B. Kaplan, K.L. Brayman, Prospective investigations of concentration–clinical response for immunosuppressive drugs provide the scientific basis for therapeutic drug monitoring, Clin. Chem. 44 (1998) 381–387. https://doi.org/10.1093/clinchem/44.2.381.
[22] A. Johnston, D.W. Holt, Therapeutic drug monitoring of immunosuppressant drugs, Br. J. Clin. Pharmacol. 47 (1999) 339–350. https://doi.org/10.1046/j.1365-2125.1999.00911.x.
[23] M. Regazzi, J. Golay, M. Molinaro, Monoclonal antibody monitoring: clinically relevant aspects, a systematic critical review, Ther. Drug Monit. 42 (2020) 45–56. https://doi.org/10.1097/FTD.0000000000000681.
[24] M. Ovacik, K. Lin, Tutorial on monoclonal antibody pharmacokinetics and its considerations in early development, Clin. Transl. Sci. 11 (2018) 540–552. https://doi.org/10.1111/cts.12567.
[25] A. Patton, M.C. Mullenix, S.J. Swanson, E. Koren, An acid dissociation bridging ELISA for detection of antibodies directed against therapeutic proteins in the presence of antigen, J. Immunol. Methods. 304 (2005) 189–195. https://doi.org/10.1016/j.jim.2005.06.014.
[26] R. Pai, N. Ma, A.V. Connor, D.M. Danilenko, J.M. Tarrant, D. Salvail, L. Wong, D.P. Hartley, D. Misner, E. Stefanich, Y. Wu, Y. Chen, H. Wang, D.M. Dambach, Therapeutic antibody-induced vascular toxicity due to off-target activation of nitric oxide in cynomolgus monkeys, Toxicol. Sci. 151 (2016) 245–260. https://doi.org/10.1093/toxsci/kfw037.
[27] How to Run an R&D Systems Luminex® Assay, Www.Rndsystems.Com. https://www.rndsystems.com/resources/protocols/how-run-rd-systems-luminex-assay (accessed January 25, 2021).
[28] D.H. Wilson, D.M. Rissin, C.W. Kan, D.R. Fournier, T. Piech, T.G. Campbell, R.E. Meyer, M.W. Fishburn, C. Cabrera, P.P. Patel, E. Frew, Y. Chen, L. Chang, E.P. Ferrell, V. von Einem, W. McGuigan, M. Reinhardt, H. Sayer, C. Vielsack, D.C. Duffy, The Simoa HD-1 Analyzer: a novel fully automated digital immunoassay analyzer with single-molecule sensitivity and multiplexing, J. Lab. Autom. 21 (2016) 533–547. https://doi.org/10.1177/2211068215589580.
[29] K.N. Han, C.A. Li, G.H. Seong, Microfluidic chips for immunoassays, Annu. Rev. Anal. Chem. 6 (2013) 119–141. https://doi.org/10.1146/annurev-anchem-062012-092616.
[30] A.H.C. Ng, U. Uddayasankar, A.R. Wheeler, Immunoassays in microfluidic systems, Anal. Bioanal. Chem. 397 (2010) 991–1007. https://doi.org/10.1007/s00216-010-3678-8.
[31] M. Zalis, C.L. Jaffe, Routine dot-blot assay of multiple serum samples using a simple apparatus, J. Immunol. Methods. 101 (1987) 261–264. https://doi.org/10.1016/0022-1759(87)90158-X.
[32] N. Cardona-Castro, P. Agudelo-Flórez, Immunoenzymatic dot-blot test for the diagnosis of enteric fever caused by Salmonella typhi in an endemic area, Clin. Microbiol. Infect. 4 (1998) 64–69. https://doi.org/10.1111/j.1469-0691.1998.tb00357.x.
[33] S. Ramachandran, M. Singhal, K.G. McKenzie, J.L. Osborn, A. Arjyal, S. Dongol, S.G. Baker, B. Basnyat, J. Farrar, C. Dolecek, G.J. Domingo, P. Yager, B. Lutz, A rapid,

multiplexed, high-throughput flow-through membrane immunoassay: a convenient alternative to ELISA, Diagnostics. 3 (2013) 244–260. https://doi.org/10.3390/diagnostics3020244.
[34] P. Chen, M. Gates-Hollingsworth, S. Pandit, A. Park, D. Montgomery, D. AuCoin, J. Gu, F. Zenhausern, Paper-based Vertical Flow Immunoassay (VFI) for detection of bio-threat pathogens, Talanta. 191 (2019) 81–88. https://doi.org/10.1016/j.talanta.2018.08.043.
[35] Y. Jiao, C. Du, L. Zong, X. Guo, Y. Han, X. Zhang, L. Li, C. Zhang, Q. Ju, J. Liu, H.-D. Yu, W. Huang, 3D vertical-flow paper-based device for simultaneous detection of multiple cancer biomarkers by fluorescent immunoassay, Sens. Actuators B Chem. 306 (2020) 127239. https://doi.org/10.1016/j.snb.2019.127239.
[36] A.G. Berger, S.M. Restaino, I.M. White, Vertical-flow paper SERS system for therapeutic drug monitoring of flucytosine in serum, Anal. Chim. Acta. 949 (2017) 59–66. https://doi.org/10.1016/j.aca.2016.10.035.
[37] H.Y. Tan, J. Yang, J.C. Linnes, C.J. Welch, M.L. Bruening, Quantitation of trastuzumab and an antibody to SARS-CoV-2 in minutes using affinity membranes in 96-well plates, Anal. Chem. 94 (2022) 884–891. https://doi.org/10.1021/acs.analchem.1c03654.
[38] W. Liu, A.L. Bennett, W. Ning, H.-Y. Tan, J.D. Berwanger, X. Zeng, M.L. Bruening, Monoclonal antibody capture and analysis using porous membranes containing immobilized peptide mimotopes, Anal. Chem. 90 (2018) 12161–12167. https://doi.org/10.1021/acs.analchem.8b03183.
[39] H.M. Geysen, S.J. Rodda, T.J. Mason, A priori delineation of a peptide which mimics a discontinuous antigenic determinant, Mol. Immunol. 23 (1986) 709–715. https://doi.org/10.1016/0161-5890(86)90081-7.
[40] C. Liedert, L. Rannaste, A. Kokkonen, O.-H. Huttunen, R. Liedert, J. Hiltunen, L. Hakalahti, Roll-to-roll manufacturing of integrated immunodetection sensors, ACS Sens. 5 (2020) 2010–2017. https://doi.org/10.1021/acssensors.0c00404.
[41] H. Becker, C. Gärtner, Polymer microfabrication technologies for microfluidic systems, Anal. Bioanal. Chem. 390 (2008) 89–111. https://doi.org/10.1007/s00216-007-1692-2.
[42] T.J. Moehling, D.H. Lee, M.E. Henderson, M.K. McDonald, P.H. Tsang, S. Kaakeh, E.S. Kim, S.T. Wereley, T.L. Kinzer-Ursem, K.N. Clayton, J.C. Linnes, A smartphone-based particle diffusometry platform for sub-attomolar detection of Vibrio cholerae in environmental water, Biosens. Bioelectron. 167 (2020) 112497. https://doi.org/10.1016/j.bios.2020.112497.
[43] J. Dai, G.L. Baker, M.L. Bruening, Use of porous membranes modified with polyelectrolyte multilayers as substrates for protein arrays with low nonspecific adsorption, Anal. Chem. 78 (2006) 135–140. https://doi.org/10.1021/ac0513966.
[44] S. Bhattacharjee, J. Dong, Y. Ma, S. Hovde, J.H. Geiger, G.L. Baker, M.L. Bruening, Formation of high-capacity protein-adsorbing membranes through simple adsorption of poly(acrylic acid)-containing films at Low pH, Langmuir. 28 (2012) 6885–6892. https://doi.org/10.1021/la300481e.
[45] S. Wijeratne, W. Liu, J. Dong, W. Ning, N.D. Ratnayake, K.D. Walker, M.L. Bruening, Layer-by-layer deposition with polymers containing nitrilotriacetate, a convenient route to fabricate metal- and protein-binding films, ACS Appl. Mater. Interfaces. 8 (2016) 10164–10173. https://doi.org/10.1021/acsami.6b00896.

[46] N. Anuraj, S. Bhattacharjee, J.H. Geiger, G.L. Baker, M.L. Bruening, An all-aqueous route to polymer brush-modified membranes with remarkable permeabilites and protein capture rates, J. Membr. Sci. 389 (2012) 117–125. https://doi.org/10.1016/j.memsci.2011.10.022.
[47] J.D. Berwanger, H.Y. Tan, G. Jokhadze, M.L. Bruening, Determination of the serum concentrations of the monoclonal antibodies bevacizumab, rituximab, and panitumumab using porous membranes containing immobilized peptide mimotopes, Anal. Chem. (2021). https://doi.org/10.1021/acs.analchem.0c04903.
[48] B.L. Boyanton, Jr., K.E. Blick, Stability studies of twenty-four analytes in human plasma and serum, Gen. Clin. Chem. 48 (2002) 2242–2247.
[49] Bevacizumab ELISA Kit (ab237642) | Abcam, https://www.abcam.com/bevacizumab-elisa-kit-ab237642.html (accessed August 8, 2022).

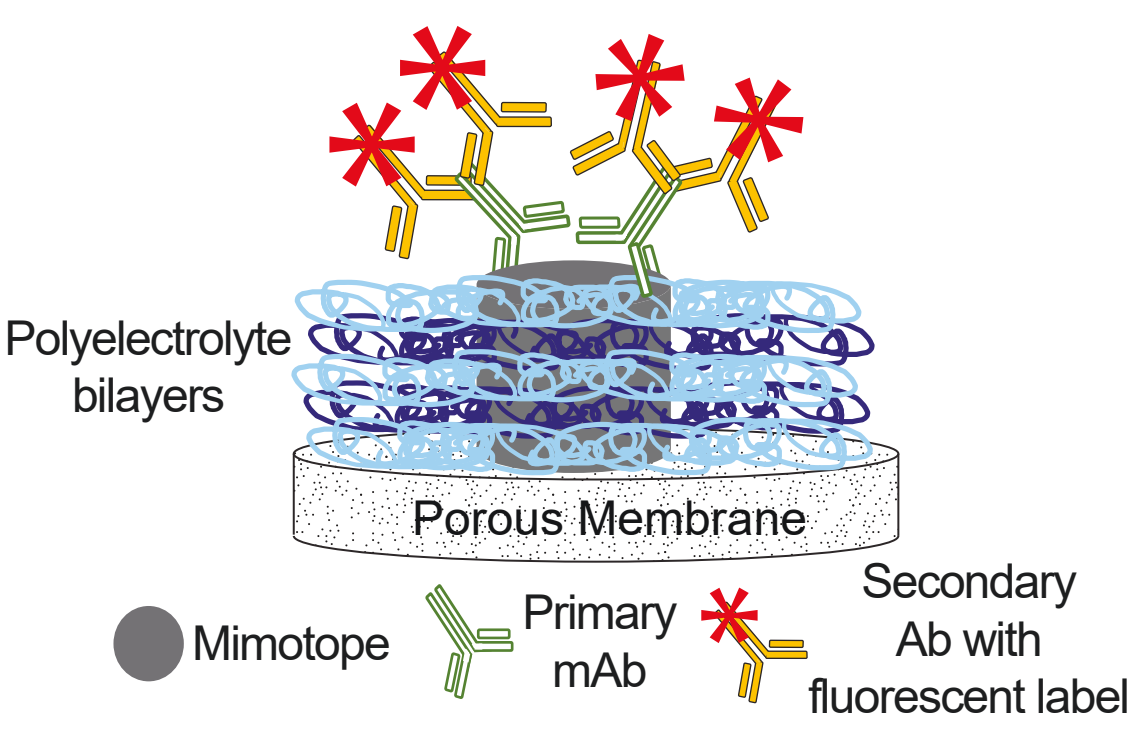
Polyelectrolyte bilayers
Porous Membrane
Mimotope
Primary mAb
Secondary Ab with fluorescent label

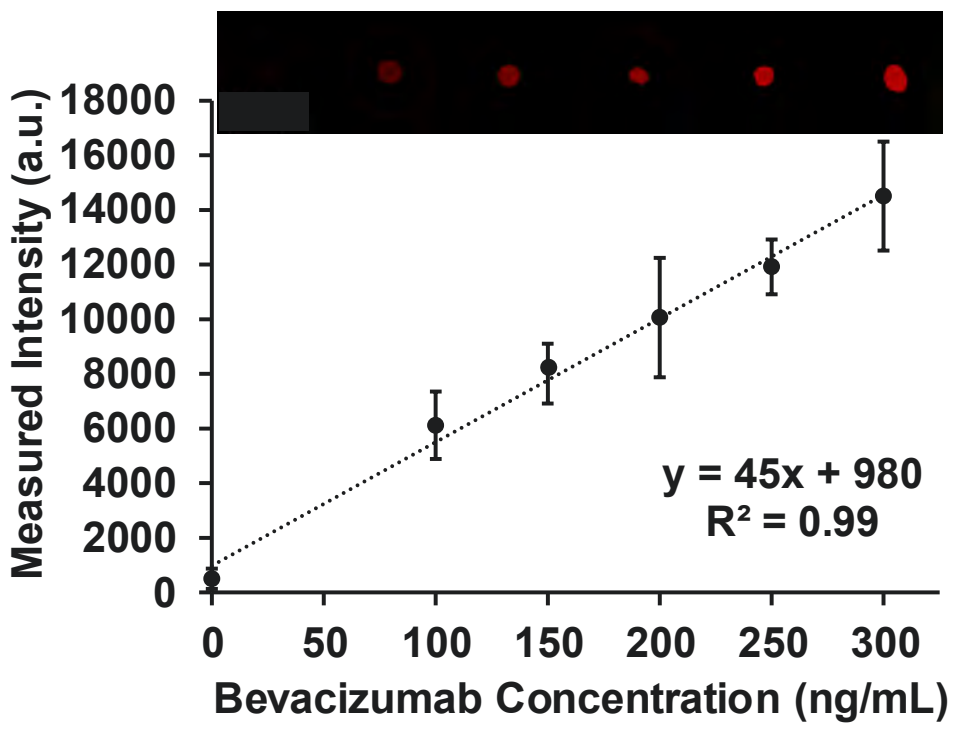
Measured Intensity (a.u.)
18000
16000
14000
12000
10000
8000
6000
4000
2000
0
0
50
100
150
200
250
300
Bevacizumab Concentration (ng/mL)
y = 45x + 980
R² = 0.99